Energy 123 (2017) 314–325

Contents lists available at ScienceDirect

Energy

journal homepage: www.elsevier.com/locate/energy

Cost-based design optimization of the heat exchangers in a parabolic trough power plant

P.A. González-Gómez*, F. Petrakopoulou, J.V. Briongos, D. Santana

Department of Thermal and Fluid Engineering, University Carlos III of Madrid, Campus of Leganes, 28911 Madrid, Spain

ARTICLE INFO

Article history:
Received 6 June 2016
Received in revised form
31 January 2017
Accepted 1 February 2017
Available online 2 February 2017

Keywords:
Solar thermal power plant
Parabolic trough
Thermal energy storage
Steam generator
Heat exchanger design
Design optimization

ABSTRACT

This paper addresses two important concerns of the design of steam generators of parabolic trough power plants: cost minimization and component reliability. A thorough economic analysis of the heat exchangers of the steam generator and oil-to-salt heat exchangers of a 50 MWe parabolic trough power plant is presented. The heat exchanger design is realized following TEMA standards and optimized using a genetic algorithm. Two design strategies are compared: the minimization of the total heat transfer area and the minimization of the total annualized cost. It is seen that the second approach provides substantial savings over the lifetime of the plant.

The economic analysis reveals a global optimum with an outlet temperature of the heat transfer fluid of 293 °C and an evaporator pinch point of 4.85 °C. The best design of the steam generator consists of a TEMA-H shell superheater and preheater and a TEMA-F shell reheater. The best design of the oil-to-salt heat exchangers includes six TEMA-F shell heat exchangers in series, with a log mean temperature difference of 7 °C and the molten salt on the shell-side. Lastly, a TEMA-X recirculation evaporator is proposed with a considerably reduced wall thickness when compared to a kettle evaporator.

1. Introduction

Concentrating solar power (CSP) plants have regained scientific attention recently, after 20 years of stagnation. This was mainly driven by government subsidies and technological advances. In addition, thermal storage allows CSP plants to participate in electricity markets that increase their economic competitiveness [1]. The majority of the commercial CSP plants constructed in Spain include a 50 MWe steam Rankine cycle, with a solar multiple of 2 and 7.5 h of storage [2]. Until today, CSP plants of a total capacity of 4 GW have been installed worldwide (around 90% of them are based on parabolic trough technology). The International Energy Agency (IEA) estimates an increase of the global CSP capacity to 1000 GW by 2050 [3].

The design of a heat exchanger used in energy systems is realized in two steps: a) heat transfer and pressure drop calculation and b) cost analysis and optimization realization. Heat transfer and pressure drop calculations can be found in several published works in literature. The majority of these publications use the Bell-Delaware method for shell side calculations [4–6]. In contrast, one of the most utilized commercial software for heat exchanger design (Heat Transfer Research Inc. (HTRI) software) is based on the principles of the Stream Analysis method [7]. Simplified economic analyses of heat exchangers are published in numerous studies [8–10]. Purohit [11] proposed a thorough method to estimate the purchase cost of heat exchangers based on the Tubular Exchanger Manufacturers Association (TEMA) standards. Cost minimization of heat exchangers involves the selection of different geometric parameters (e.g., shell and tube diameters, tube layout and pitch, the number of tubes, baffle spacing) subject to different design constraints. To minimize the cost, optimization methods such as genetic algorithms (GA), particle swarm optimization and others can be used. Wildi-Tremblay and Gosselin [12] used a GA to minimize the total annual investment and operational cost of a shell and tube heat exchanger. They showed that the GA found the optimal design of eleven design variables 23 times faster than the time required to evaluate all possible combinations. Ponce et al. [13] developed a penalty function to quantify the violation level of heat exchanger design constraints, improving the performance of the GA. Fettaka el al [14]. performed a multi-objective optimization using a fast and elitist non-dominated sorting genetic algorithm (NSGA-II) to minimize the area and total pressure drop of heat exchangers. They

* Corresponding author.
E-mail address: pegonzal@ing.uc3m.es (P.A. González-Gómez).

http://dx.doi.org/10.1016/j.energy.2017.02.002
0360-5442/

Nomenclature

Abbreviations

CF	capacity factor
CT	cold tank
EV	evaporator
FW	feed water
HP	high pressure
HTF	heat transfer fluid
HT	hot tank
LP	low pressure
LCOE	levelized cost of electricity (€/kWh)
LMTD	log mean temperature difference (°C)
PB	power block
PH	preheater
RH	reheater
SF	solar field
SG	steam generator
SH	superheater
TAC	total annualized cost (€/year)
TES	thermal energy storage

Symbols

A	heat transfer area (m^2)
B_c	baffle cut (−)
C	cost (€)
CE_{index}	Chemical Engineering Plant Cost Index (−)
Cp	specific heat capacity (J/kg °C)
D	diameter (m)
E	energy (kWh/year)
F	log mean temperature difference correction factor (−)
F_b	bundle heat transfer correction factor (−)
F_{tp}	Two phase heat transfer correction factor (−)
G_c	critical mass flux (kg/m^2 s)
H	height (m)
H_y	annual plant operation time (h/year)
K	resistance coefficient (−)
L	length (m)
L_{bc}	baffle spacing (m)
N_{cold}	number of cold starts
N_{hot}	number of hot starts
N_{tp}	number of tube passes (−)
N_{tt}	number of tubes (−)
N_s	number of shells (−)
P	pressure (Pa)
R	fouling resistance (°C m^2/W)
S	stream flow area (m^2)
SA	dome segment area (m^2)
T	temperature (°C)
U	global heat transfer coefficient (W/m^2 °C)
VL	vapor load parameter (kg/s m^3)
W	weight (kg)
$W_{turbine}$	turbine power (MWe)
b	cost of baseline heat exchanger (EUR/m^2)
c_1 to c_3	cost law coefficients
c_f	chocking correction factor (−)
f	cost multiplier for TEMA-type front head (−)
g	gravity acceleration (m/s^2)
h	convective coefficient (W/m^2 °C)
l_{ts}	tubesheet thickness (mm)
$\dot{m}$	mass flow rate (kg/s)
p	cost multiplier for tube outside diameter, pitch and layout (−)
pc	penalty coefficient (−)
pp	pinch point (°C)
r	cost multiplier for TEMA-type rear head (−)
t_s	shell thickness (m)
v	velocity (m/s)
$\mathbf{x}$	vector of optimization variables (−)
$\mathbf{y}$	vector of feasible constraints (−)

Greek symbols

α	suppression factor (−)
δ	temperature profile distortion factor (−)
η_{PB}	power block efficiency (−)
θ_{tp}	tube layout (°)
ρ	density (kg/m^3)
ϕ_v	viscosity correction factor (−)

Subscripts

d	drum
dc	downcomer
dp	driving pressure
fm	frictional and momentum
fc	forced convection
hx	heat exchanger
invest	investment
nb	nucleate boiling
nc	natural convection
l	liquid phase
o	thermal oil
om	operation and maintenance
out	outlet.
pl	platforms
r	riser
ref	reference condition
s	shell
t	outside of tube
ti	inside of tube
tp	two phase

also studied the impact on the optimal design when selected geometric parameters are used either in a discrete or continuous form.

Until today, several studies that estimate the size of SG and oil-to-salt heat exchangers of parabolic trough power plants have been published. For example, Kelly [15] analyzed the impact of the capacity of a CSP plant on the energy cost and presented the layout, surface areas and cost of the SG heat exchangers of a 250 MWe CSP plant. Kelly and Kearney [16] optimized an indirect molten salt thermal energy storage (TES) and realized a preliminary SG sizing. They presented an SG design of counter-current heat exchangers and estimated the corresponding surface areas and pressure drops. The TES optimization was realized through the sizing of the oil-to-salt heat exchanger, because it affects the total size of the TES system, as well as the performance of the turbine. Cost calculations were realized for the different parts of the storage system, including the oil-to-salt heat exchanger. Herrmann et al. [17] proposed a conventional shell-and-tube design as an economical solution for oil-to-salt heat exchangers. They calculated different heat

exchanger sizes for various storage capacities taking into account the heat duty required during charging and discharging. Zaversky et al. [18] proposed an oil-to-salt heat exchanger design with two tube passes and two shell passes and studied its transient response. Although, some heat exchanger design calculations are available in this work, information about velocities, pressure drops and costs is missing. It is thus seen overall that detailed heat exchanger design calculations of SG and oil-to-salt heat exchangers are still not available in literature. The present work aims to address this issue.

This paper presents the design and the economic analysis of the SG and oil-to-salt heat exchangers of a 50 MWe parabolic trough solar power plant. The results presented are based on the Stream Analysis method using Wills and Johnston version [7]. The economic analysis follows the methodology proposed by Purohit [11]. For the SG, different evaporator pinch points and heat transfer fluid (HTF) outlet temperatures are studied, bearing in mind the total operational cost. An alternative recirculation evaporator is modeled and compared with a kettle evaporator. Furthermore, the impact of different oil-to-salt heat exchanger approach temperatures on the performance of the power block is analyzed under TES discharging conditions. The analysis is carried out taking into account the total TES cost and the associated cost power block efficiency penalty. The proposed designs of the SG and oil-to-salt heat exchangers follow TEMA standards. Lastly, a GA, following the model developed by Ponce et al. [13], is used to find the optimal heat exchanger design.

2. Methodology

2.1. Calculation of heat transfer and pressure drops in the heat exchangers

In this work, the Stream Analysis method was chosen for the shell-side calculations in the single-phase heat exchangers. A qualitative analysis of the Stream Analysis method is presented by Palen and Taborek [19]. Since, the values of many empirical parameters and correlations are confidential in the HTRI software, simplified correlations developed by Wills and Johnston [7] were used here to calculate the shell-side flow distribution.

In the Stream Analysis method, the shell side flow is divided into six different sub-streams: the tube-to-baffle leakage (A), the cross flow (B), the bundle-to-shell bypass (C), the shell-to-baffle leakage (E) and the tube-pass-partition bypass (F). The pressure drop of each stream in one baffle can be expressed as:

$$\Delta P_j = \frac{K_j (\dot{m}_j / S_j)^2}{2\rho\phi_v} \quad j = A, B, C, E, F \tag{1}$$

with, $\dot{m}_j$, S_j and K_j the mass flow rate, flow area and resistance coefficient for each j stream, respectively, and ϕ_v the viscosity correction factor equal to $(\mu/\mu_w)^{0.14}$. The system of equations can be solved by means of an iterative process. The system converges when achieving the same pressure drop on the meeting points in an ideal baffle hydraulic network. The different streams have different temperature profiles along the heat exchanger. Thus, it is necessary to correct both the log mean temperature difference (LMTD) and the correction factor for LMTD (F), with a temperature profile distortion factor (δ). In this way, the mean temperature difference is:

$$\Delta T_m = \delta\, F\, LMTD \tag{2}$$

The distortion temperature profile effect can be quantified using an empirical correlation [19]. In this work, all designs have been realized with recommended shell-to-baffle clearances and turbulent flow regime. Under these conditions, δ can be considered to be close to 1.

The heat transfer coefficient on the shell side can be estimated with an empirical correlation function of the Reynolds number based on cross flow stream [20].

The total pressure drop on the shell side can be expressed in terms of the pressure drop in the cross-flow zone, windows zone and the nozzles:

$$\Delta P_s = \Delta P_{cross}(N_b + 1) + \Delta P_{window}(N_b) + \Delta P_{nozzle,in} + \Delta P_{nozzle,out} \tag{3}$$

The tube side heat transfer coefficient is determined using the Gnielinski correlation [7], while the Darcy friction factor for pressure drop is calculated using the Colebrook correlation [7].

The shell-side heat transfer coefficient in the kettle evaporator (Equation (4)) was estimated considering the nucleate boiling heat transfer coefficient ($h_{nb,1}$) for a single tube and corrected with the bundle geometry factor (F_b) and the natural convective coefficient (h_{nc}) [21].

$$h_s = h_{nb,1} F_b + h_{nc} \tag{4}$$

For the shell side heat transfer coefficient in a recirculation evaporator, in addition to nucleate boiling and natural convective, is necessary take into account the forced convection due to high circulation flow rates. The forced convection heat transfer coefficient for a two-phase fluid is determined as follows:

$$h_{fc} = h_l\, F_{tp} \tag{5}$$

where, h_l is the liquid-phase heat transfer coefficient and F_{tp} is the two phase factor. The model proposed by Swanson and Palen [22] for the shell side boiling heat transfer coefficient in shell and tube heat exchangers considers the three previously mentioned mechanisms. Thus, the shell side coefficient becomes:

$$h_s = \alpha\, h_{nb} + h_{nc} + h_{fc} \tag{6}$$

where, α is the nucleate boiling suppression factor, $0 \le \alpha \le 1$.

The driving pressure (Equation (7)) is produced by the density difference between the two-phase mixture in the riser (r) and downcomer (dc) tubes. An important factor when designing natural circulation boilers is the height of the downcomer and the riser because it affects the available driving pressure.

$$\Delta P_{dp} = g\, \rho_{dc} H_{dc} - g(\rho_{hx} H_{hx} + \rho_r H_r) \tag{7}$$

The frictional and momentum (fm) pressure drop is calculated as the pressure drop in the circulation loop of the downcomer, heat exchangers (hx), riser and nozzles (Equation (8)).

$$\Delta P_{fm} = \Delta P_{dc} + \Delta P_{hx} + \Delta P_r + \Delta P_{nozzles} \tag{8}$$

Because the calculation procedure couples fluid dynamics with heat transfer, it is necessary to solve the problem by means of an iterative process. First, the evaporator heat transfer area is estimated based only on the nucleate boiling because at this point the circulation rate is unknown and the nucleate boiling is not a function of the mass flow. The evaporator geometric layout can be estimated afterwards. Second, a trial circulation rate is selected to solve the fluid dynamics equation system (Equations (7) and (8)). This step is solved when all frictional pressure drops equals the available driving pressure. At this point, the new evaporator heat transfer area and layout is calculated taking into account the convective boiling produced by the circulation rate estimated in the last iteration. The process is repeated until fluid dynamics and heat transfer convergence is achieved.

2.2. Economic analysis

The design feasibility of the heat exchangers is evaluated with an economic analysis. In this work, the total annualized cost (TAC) was used as the objective function of the optimization process [4,13,23]. The expression for total annual cost is:

$$TAC = frc\, C_{capital} + C_{operation} \tag{9}$$

$$C_{capital} = C_{hx} + C_{pump} \tag{10}$$

$$C_{operation} = C_{power}\frac{H_y}{\eta_{pump}}\left(\frac{\dot{m}_t \Delta P_t}{\rho_t} + \frac{\dot{m}_s \Delta P_s}{\rho_s}\right) \tag{11}$$

where, frc is the annuity factor, C_{hx} and C_{pump} are the investment costs of the heat exchangers and pumps, respectively, and $C_{operation}$ is the cost of the power that drives the pumps. To calculate this cost the annual operating hours (H_y) must be known. When the operating hours are not known, a reasonable approximation is made multiplying 8760 with the solar plant capacity factor (CF). The solar capacity factor is defined as the ratio between the net energy produced in one year and the energy that could have been produced at full-load conditions [24].

According to Hall et al. [8], the investment cost of a heat exchanger can be estimated using Equation (12). c_1, c_2 and c_3 are the cost law coefficients and A is the surface area of the heat exchanger. This model reflects economies of a scale typically found in chemical process plants.

$$C_{hx} = c_1 + c_2 A^{c_3} \tag{12}$$

A more detailed method proposed by Purohit [11] was used here to calculate the investment cost of heat exchangers. This method is relatively complex because it takes into account many input parameters:

$$C_{hx} = \frac{CE_{index}}{CE_{index,ref}}\left(b\cdot\left(1 + \sum_{i=1}^{N_{inputs}} c_i\right)\cdot A \cdot N_s\right) \tag{13}$$

where, CE_{index} is the Chemical Engineering Plant Cost Index, c_i is a correction factor for input i (e.g., tube/shell material, pressure work, etc.), N_s is the number of shells and b is the base cost. The base cost can be expressed as:

$$b = \left(\frac{6.6}{1 - e^{\left(\frac{(7-D_s)}{27}\right)}}\right) p\, f\, r \tag{14}$$

where, D_s is the internal diameter of the shell, p is the cost multiplier of the tube outside diameter, pitch and layout angle, f is the cost multiplier of the TEMA front head type and r is the cost multiplier of the TEMA rear head type.

The cost of the steam drum of the recirculation evaporator can be estimated as a function of the drum metal mass [9].

It should be mentioned that an economic evaluation based on TAC does not take into account all of the costs that may influence the optimum design. For example, each outlet temperature of the power block results in a different thermal oil mass flow in the solar field, and consequently to different pressure drops and pump consumptions. In order to take into account all of the former mentioned costs using standard criteria, the calculation of the levelized cost of energy (LCOE) is required.

$$LCOE = \frac{fcr\, C_{invest} + C_{om} + C_{fuel}}{E_{net}} \tag{15}$$

where, C_{invest} is the total investment cost of the plant, C_{om} the annual operational and maintenance costs and C_{fuel} is the cost of the annual use of fuel. These costs have been estimated using data provided by Montes et al. [25]. Since in this work, the considered CSP plant does not include a fossil fuel back-up system, the annual fuel costs are zero. The annual net electric energy produced E_{net}, was calculated subtracting the annual parasitic losses:

$$E_{net} = E_{gross} - E_{start,SG} - E_{pump,SF} - E_{pump,SG} \tag{16}$$

where $E_{start,SG}$ is the annual start-up energy consumption required to warm-up the metal mass of the heat exchangers and $E_{pump,SF}$ and $E_{pump,SG}$ are the annual pump consumptions of the solar field and the SG, respectively.

The investment cost of the TES system was estimated using literature data [3,16]. The cost of the hot and cold tanks, the quantity of the molten nitrate salt and the balance of the storage system were extrapolated as functions of the storage equivalent hours to full load capacity hours. The cost of the nitrate salt pumps was calculated according to the correlation proposed by Kelly and Kearney [16]. The investment cost of the oil-to-salt heat exchanger was estimated using the Purohit method.

2.3. Genetic algorithm

The large number of variables and constraints involved in the design of the heat exchangers of the SG cannot be handled by a traditional trial-and-error design method. To obtain improved designs, optimization tools must be used. Commonly used optimization methods for shell and tube heat exchangers are genetic algorithms (GA). The procedure consists of generating an initial population from random variables. Then, crossover and chromosome mutation factors are used to generate a new generation, evaluated by the objective function. This process is repeated until the GA achieves specified criteria.

The fitness function includes the TAC and the penalty function and it is expressed as:

$$fitness(\mathbf{x}) = TAC(\mathbf{x}) + penalty(\mathbf{x}) \tag{17}$$

where, $\mathbf{x}$ is the vector of design variables used to minimize the fitness function. The penalty function, defined to provide an efficient performance is expressed as [13]:

$$penalty(\mathbf{x}) = \begin{cases} 0 & if\ \mathbf{x}\ is\ feasible \\ \sum_{i=1}^{N} pc_i\, y_i^2(\mathbf{x}) & otherwise \end{cases} \tag{18}$$

where, pc_i is a penalty coefficient that varies with each generation and y_i corresponds to the level of constraint violation. The heat exchanger design variables are shown in Table 1.

The optimization parameters of the GA were the following: population size of 100 individuals with an elite count of three individuals, crossover fraction of 0.7 and mutation rate of 0.1. Two stopping criteria were used: the stall generation limit (when no further improvements are observed), which was set to 20; and the maximum number of generations, which was set to 300.

3. Initial design of the parabolic trough plant

In this work, a parabolic trough power plant with 7.5 storage

Table 1
Design variables.

Variable	Single-phase heat exchanger	Evaporator
x_1	Shell diameter	Shell diameter
x_2	Tube diameter	Tube diameter
x_3	Tube layout (triangular, square or rotated square)	Tube layout (triangular, square or rotated square)
x_4	Tube pitch	Tube pitch
x_5	Number of shells	Number of shells
x_6	TEMA shell (E, F or H)	Recirculation ratio (for Kettle = 0)
x_7	Shell side velocity	Tube side velocity
x_8	Tube side velocity	–
x_9	Baffle cut	–

hours and a solar multiple of 2 is assumed. A schematic of the parabolic trough CSP plant is shown in Fig. 1. The plant can be divided into four subsystems: the solar field, the SG, the power block and the TES system. The solar field is composed of parabolic collector sets in parallel loops that concentrate the solar irradiation for heating the thermal oil as heat transfer fluid. Normally, the thermal oil works at temperatures below 400 °C in order to prevent fluid degradation. Here, the thermal oil is heated in the solar field to a temperature of 393 °C ($T_{SF,OUT}$). The SG includes the generation train: superheater (SH), evaporator (EV) and preheater (PH) connected in parallel with the reheat train (reheater, RH). Thermal oil flows through the SG to supply the thermal energy to increase the temperature from the exit water of the last feedwater heater to the high-pressure turbine inlet steam. The power block of the plant is based on a regenerative Rankine cycle with single reheat and extractions to the feedwater heaters. The working fluid of the cycle is water, the live steam pressure and temperature are 106 bar and 377 °C ($T_{HP,IN}$) and the reheat steam temperature is 378 °C ($T_{LP,IN}$). The gross power output of the turbine is 55 MWe and the nominal efficiency of the power block is 37.5%. The excess of thermal energy produced in the solar field is sent to the thermal energy storage (TES) unit of the facility. The TES system consists of two molten salt tanks (one cold and one hot), where the hot and cold molten salt is stored in the hot and cold tanks, respectively. Thermal energy is transferred from the thermal oil to the molten salt (charging) and the opposite (discharging) in the oil-to-salt heat exchanger.

The System Advisor Model (SAM) [26] was used to estimate the annual gross energy E_{gross} and the power pump consumption of the solar field $E_{pump,SF}$. The annual start-up energy was estimated as:

$$E_{start,SG} = W_{hx}\, Cp_w (N_{hot}\Delta T_{hot} + N_{cold}\Delta T_{cold})\eta_{PB} \quad (19)$$

where, W_{hx} is the weight of the heat exchangers, Cp_w is the specific heat capacity, η_{PB} is the efficiency of the power block and N_{hot} and N_{cold} are the number of the annual hot and cold start-ups, respectively. A start-up is considered hot when the metal temperature (measured in the turbine unit before the start-up) is at 80% the nominal temperature. In cold start-ups, the metal temperature falls below 60% of the nominal temperature. According to Guédez et al. [27], the number of start-ups for a standard parabolic trough plant is 365 per year. Approximately 70% of those are hot starts. In this work, we considered the same cooling evolution for the SG heat exchangers as that considered by Guedez et al. [27].

Nominal values of the Rankine cycle are shown in Table 2. Thermodynamic properties of the water and steam streams are calculated based on analytical formulas for absolute and derivative values [28]. Thermal oil properties are selected based on data presented in Ref. [26].

4. Mechanical design and TEMA standards

TEMA standards provide guidelines for shell and tube heat exchanger components, such as: shell type, front head type, rear head type, outside tube diameters, maximum and minimum baffle spacing, clearances, baffle thickness, maximum tube length, fouling factors, tubesheet thickness and others [29]. In this work, the mechanical design was carried out for selected elements of the heat exchangers. Shell and tube thicknesses were calculated according to the ASME code (section VIII and II, respectively) and compared to the minimum thicknesses recommended by TEMA. Baffle thicknesses, tube sheet thicknesses and clearances (shell-baffle, tube-baffle and bundle-shell) were calculated according to TEMA. In addition, the material selected for the shell and plates was ASTM A516 Grade 70 carbon steel. For the tubes ASTM A192 carbon steel was selected [30].

Conventional shell and tube heat exchangers were selected for the oil-to-salt and SG heat exchangers. Different TEMA shell types were modeled in order to enhance the performance of the heat exchanger. TEMA-E type is the most common and economical shell type used in chemical industries. However, this shell type does not

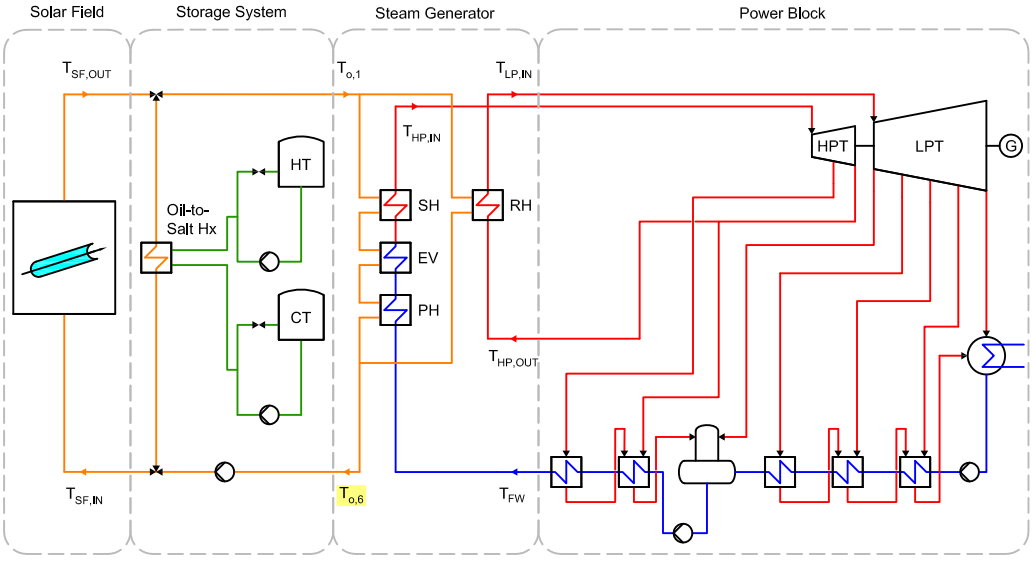

Fig. 1. Schematic of the parabolic trough solar power plant.

Table 2
Nominal values of the 55 MWe (gross) steam power cycle.

Turbine point	Pressure (bar) (T. sat, °C)	Temperature (°C)	Mass Flow (kg/s)	Steam condition
HP inlet	106	377	61.91	One phase
Extraction 1	41.33 (252.30)	260.4	6.78	One phase
HP exhaust	20.73	214.2	55.13	Two phase
Extraction 2	20.73	214.2	3.814	Two phase
Condensate Separator	–	–	1.718	–
LP inlet	18.3	378	49.69	One phase
Extraction 3	10.5 (182.01)	310.6	3.114	One phase
Extraction 4	4 (143.61)	202.4	3.09	Two phase
Extraction 5	1.3	107.1	2.096	Two phase
Extraction 6	0.536	83	2.636	Two phase
LP exhaust	0.078	41.03	39.39	Two phase

always satisfy specific process requirements. In order to improve the thermal effectiveness, a TEMA-F shell type with two tube passes is usually preferred. In this type, a longitudinal baffle divides the flow path, making it a counter-current heat exchanger and avoiding in this way temperature crossings. When a low-pressure drop is required in the shell side, different TEMA shell types may be proposed. For example, TEMA-H and G shell types reduce the pressure drop drastically when compared to F shells. However, G shells are not recommended when larger tube lengths are required [31].

Fig. 2 illustrates the TEMA shell types developed in this work for single-phase heat exchangers. To estimate the heat transfer and pressure drop in the TEMA-F and H shell types, the geometries have been adapted reducing all stream flow areas by half, when compared to the TEMA-E shell [32]. Furthermore, it is assumed that the flow leakage and conduction across the longitudinal baffle are minimized in both cases. This assumption can be made by limiting the maximum shell side pressure drop [33].

In numerous studies of CSP plants, a kettle evaporator is selected for the SG [15,16,34]. Other references propose a recirculation evaporator as a better option [35,36]. Here, both a recirculation- and kettle-type evaporators have been modeled and compared.

A kettle evaporator consists of a horizontal TEMA-K shell with tube bundle (Fig. 3). The boiling takes place on the shell side and the vapor is separated from the liquid above the tube bundle. The main advantage of the kettle type is that it is composed of a single unit and thus associated with lower cost, when compared to other types. However, the larger diameter leads to a thicker shell and consequently, to worse performance under thermal stress. In addition, the low velocity on the shell side makes the kettle susceptible to fouling.

Recirculation evaporators, also called thermosyphon reboilers, usually have TEMA-G, H or X shells [21]. The latter provides lower investment costs and pressure drops. The boiling occurs outside the tubes on the shell side fed with the two-phase fluid from the steam drum. The density difference between the downcomer and the riser induce a high natural circulation ratio (around 10 times that of the steam exiting). This leads to a higher shell side heat transfer coefficient and a small surface area when compared to the kettle type. Moreover, high circulation tends to decrease the potential fouling. The main advantage of a recirculation evaporator is its smaller shell diameter, compared to other designs. The smaller diameter reduces the shell and tubesheet wall thicknesses and improves the thermal stress behavior. The main disadvantage of this type of evaporator is the higher cost compared to the kettle type. Fig. 4 illustrates a schematic of a TEMA-X shell recirculation evaporator.

A U-tube bundle was selected mainly because it can expand or contract in response to stress differentials. In addition, the tube bundle can be removed, allowing the easy cleaning of the outer side of the tubes [37]. The U-tube bundle is mounted with a fixed tubesheet on the front end and a welded shell cover on the U-bend end [38].

In order to improve the reliability of the heat exchanger a channel integral with tubesheet TEMA-C and -N heads was selected [38]. Both head types have the channel welded to the tubesheet, while the TEMA-N head has the channel welded to the shell as well. The principal advantages of the TEMA-N head are the relatively low cost and the minimum leakage of the shell-side fluid since there are no flanged joints. Thus, it may be used with hazardous or high-pressure fluids on the shell side. The TEMA-C head allows mechanical cleaning because the shell is removable and it is thus chosen with dirty fluid flows on the shell side. In the case of high

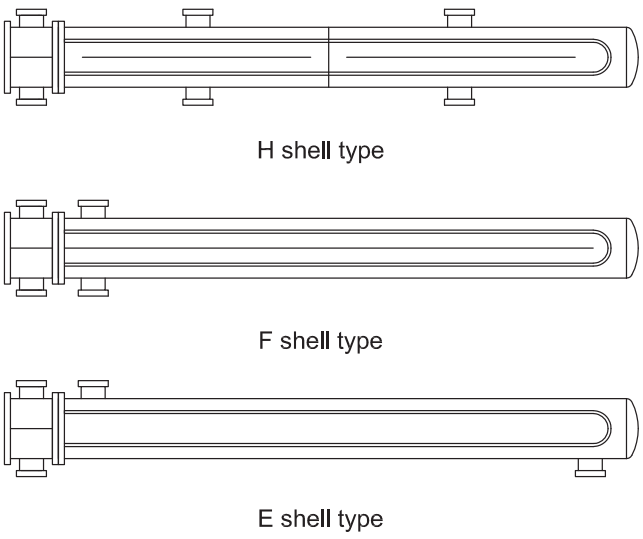

Fig. 2. TEMA shell types developed for single-phase heat exchangers.

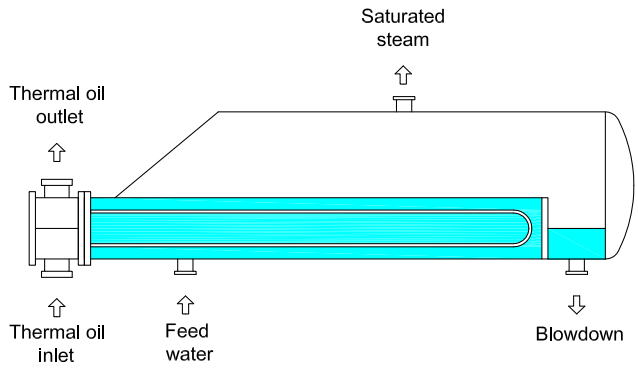

Fig. 3. Kettle type evaporator.

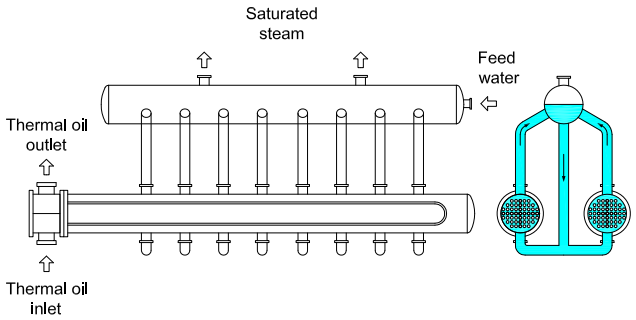

Fig. 4. TEMA-X shell recirculation evaporator.

pressure on the tube side (up to 100 bar), the TEMA-D head is selected [39].

5. Cost-based design optimization

To allow the optimization algorithm to obtain feasible designs, selected constraints based on TEMA standards and recommended good practice are used. The general heat exchanger constraints are:

1. The shell side velocity is limited between 0.2 m/s and 1.5 m/s [40].
2. The minimum tube side velocity is set to 0.5 m/s in order to reduce the fouling resistance, while the maximum is set to 4 m/s to avoid excessive erosion [40]. The maximum steam velocities are set according to the steam velocity diagram of the operational pressure, tube diameter and process type presented by Merritt [41].
3. The maximum pressure drop on the thermal oil side of the heat exchangers is set to 1.4 bar [16]. In order to prevent thermal leakage, the maximum shell-side pressure drop in H and F shells is set to 0.5 bar [33].
4. The maximum pressure drop on the water side of the heat exchangers is set to 1 bar.
5. The maximum straight tube length is set to 24 m [16]. The length for the U-tube heat exchanger is around half the straight tube length because the tubes are bent in the shape of a U.
6. The minimum baffle spacing is limited for good flow distribution and is set to the highest value between $D_s/5$ and 50 mm. The maximum baffle spacing is limited for two reasons: for proper flow distribution and to prevent sagging and possible tube vibrations.
7. The tube length to shell diameter ratio is limited between 8 and 12. Generally longer tubes with smaller diameter and thickness in shell and tubesheet are preferred [42].
8. The baffle cut limits are set as a function of the baffle spacing to shell diameter ratio [42].
9. The allowed shell-tube diameter combinations are set based on recommended practice [42]. Moreover, the minimum outside tube diameter is limited to be bigger than 14 mm, since diameters smaller than that cannot be cleaned mechanically [40].
10. Square and rotated square tube layout is preferred for thermal oil on the shell side, because a triangle layout does not allow mechanical cleaning [40].
11. In order to avoid undesirable temperature crosses [38], $F_{\min}$ is set to 0.8 in TEMA-E shells and 0.95 in TEMA-H shell designs.
12. The maximum shell side nozzle momentum is limited to 2250 kg/(s^2·m). With large mass flows, an impingement plate is added to increase the momentum to 4500 kg/(s^2·m) in an effort to decrease the diameter of the nozzle.

The design constraints applied specifically to evaporators and two-phase flows are:

1. The maximum heat flux for tube bundle is limited in order to avoid film boiling [21].
2. The critical flow (when the flow reaches the velocity of the propagation of pressure waves [43]) in water-steam mixtures is estimated using Equation (20) [44]:

$$G_c = \sqrt{2\left[P_{ref} - c_f P_{sat}\left(T_{ref}\right)\right]\rho_{l,ref}} \tag{20}$$

where, G_c is the critical mass flux, P_{ref}, T_{ref} and $\rho_{l,ref}$ are the pressure, temperature and liquid density in upstream stagnation (i.e., steam drum), respectively, and c_f is a choking correction factor.

3. As suggested for high-pressure boilers (>40 bar) [45], the circulation ratio is limited between 8 and 15.
4. The maximum shell side nozzle momentum for the two-phase flow is limited to 1500 kg/(s^2·m), in order to prevent unstable operation [42].
5. The kettle and drum diameters are chosen in order to not exceed the maximum vapor velocity that allows gravitational settling of entrained liquid droplets. The vapor load is calculated as [21]:

$$VL = 0.064\,\rho_V\left(\frac{\sigma}{\rho_l - \rho_V}\right)^{0.5} \tag{21}$$

The required dome segment area (Equation (22)) is expressed as a function of the steam mass flow ($\dot{m}_v$) and the length of the horizontal drum o kettle (L_d). Then, for a given percentage of water level (*Level*) the minimum drum or kettle diameter is given by Equation (23).

$$SA = \frac{\dot{m}_v}{L_d\,VL} \tag{22}$$

$$D_{d,\min} = \sqrt{\frac{8\,SA}{\left[2\cos^{-1}\left(\frac{2\,Level}{100} - 1\right) - \sin\left(2\cos^{-1}\left(\frac{2\,Level}{100} - 1\right)\right)\right]}} \tag{23}$$

6. The minimal number of exit nozzles is set for improving the longitudinal flow distribution along a drum or a kettle [21].

5.1. Optimizing the design of the SG

The configuration of the SG is shown in Fig. 5.The design process of the SG requires the definition of the optimal evaporator pinch point (pp_{EV}) and thermal oil outlet temperature ($T_{o,6}$). Different pp_{EV} can be obtained varying the mass flow led to the reheater train. As seen in Fig. 6, higher pp_{EV} leads to higher temperature differences in the generation train (superheater, evaporator and preheater). Consequently, the surface area of the heat exchangers decreases, reducing the associated investment cost. On the contrary, smaller temperature differences obtained in the reheat train, lead to larger heat transfer areas and higher costs. As a result, a trade-off between the costs of the generation train and the reheater is obtained (Fig. 7a). The optimal pp_{EV} is achieved when the total cost of the generation and reheat trains is minimized.

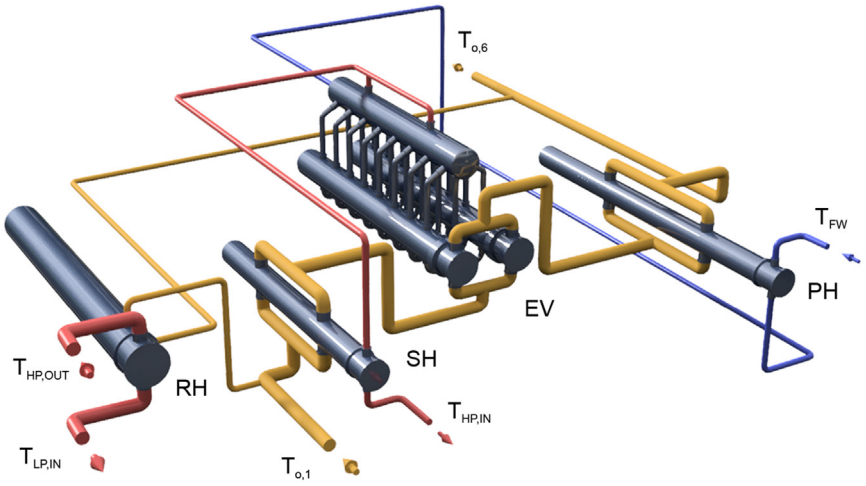

Fig. 5. SG configuration.

Since the flow rate of the thermal oil in the SG is proportional to the difference between the inlet and outlet temperatures ($T_{o,1}$ and $T_{o,6}$, respectively), if $T_{o,1}$ is kept constant, the thermal oil flow rate increases with increasing $T_{o,6}$. On the one hand, higher $T_{o,6}$ increases the power requirement of the pumps and, thus, the operational cost of the SG and the solar field. On the other hand, lower $T_{o,6}$, leads to lower temperature differences in the SG and greater heat transfer area and higher cost. In this way, a trade-off between the operational and investment costs is obtained (see Fig. 7b).

The thermal oil mass flow rate is calculated in order to supply the required heat exchanger duties at different $T_{o,6}$ ($T_{o,1}$ is kept constant at 393 °C). $T_{o,6}$ is varied from 289 to 300 °C. In all cases, the different reheater mass flows bypassed should not result in pinch points lower than 1 °C and 3 °C in the evaporator (pp_{EV}) and reheater (pp_{RH}), respectively. Then, the optimization of the SG heat exchangers was carried out individually for all combinations of pp_{EV} and $T_{o,6}$. Moreover, two optimization strategies were compared: the TAC minimization and the heat transfer area minimization.

The results of the analysis for the SG are shown Fig. 8. It can be seen that the LCOE has a higher rate of increase for higher values of pp_{EV}, due to the higher costs of the reheat train. A moderate rate of increase is obtained for lower values of pp_{EV}. The blank region in Fig. 8 corresponds to reheater pinch points lower than the minimum (infeasible cases). The optimum design corresponds to $T_{o,6}$ equal to 293 °C and pp_{EV} equal to 4.85 °C.

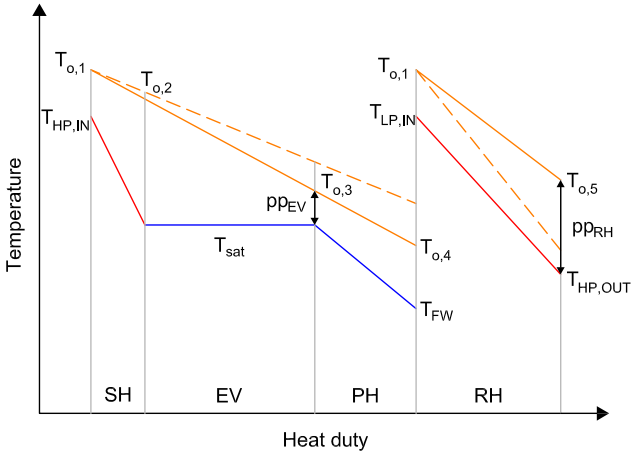

Fig. 6. SG temperatures versus heat duty.

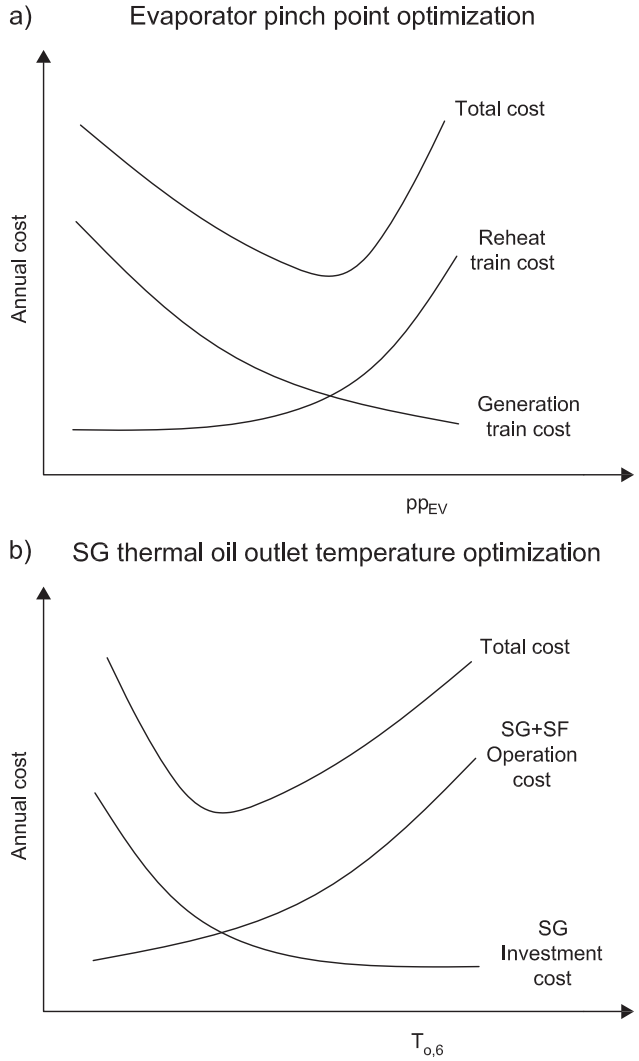

Fig. 7. SG design optimization: a) evaporator pinch point and b) thermal oil outlet temperature.

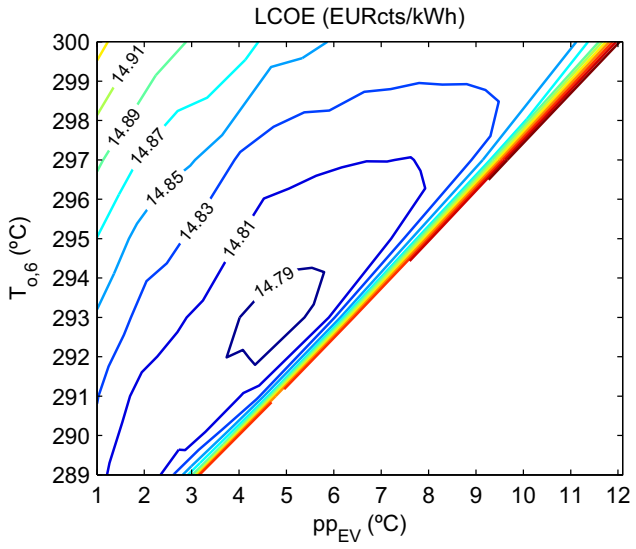

Fig. 8. Economic analysis of the SG.

Based on common practice in commercial parabolic trough plants [46,47], the SG design is optimized to include two parallel trains, each with a preheater, an evaporator, a superheater and a reheater. Initially, an SG design with one train was carried out. Although this design had lower investment cost, it led to higher wall thicknesses in the heat exchangers. Since only one train is used in this design, the complete SG system must be warmed up. This results in an increased metal mass to be heated-up and may also increase the start-up time considerably. Moreover, this design has smaller heat transfer efficiency when working at part load conditions, compared to the SG design with two parallel trains. These features may decrease the annual energy production and plant operability.

The final design characteristics of the optimized SG heat exchangers are presented in Table 3. In the superheater, the reheater and the preheater, the thermal oil is placed on the shell side and the steam or the high-pressure water on the tube side. In the evaporator, the thermal oil is placed on the tube side and the steam/water mixture on the shell side. The heat exchangers are designed with large length to diameter ratios and small wall thicknesses that can sustain the pressure. Specifically, the design of the recirculation evaporator, realized with three units (two TEMA-X shell heat exchangers and one steam drum), leads to a meaningful reduction in the shell diameter, i.e., smaller shell and tubesheet thicknesses, in comparison to a kettle. Since solar plants are subject to daily start-ups, stops and load changes, the reduction of wall thicknesses means lower thermal stress and fatigue damage. Moreover, smaller wall thicknesses allow high temperature gradients and smaller start-up time. The latter is very important for CSP plants because it leads to reduced start-up costs and increases the efficiency [48]. Furthermore, smaller wall thicknesses involve a considerable reduction in metal mass and save energy during the warm-up process.

When TAC minimization strategy is used, the algorithm solution tends to lower velocities on the thermal oil side in order to decrease the operational cost from the pressure drop in the SG. Some studies found in literature assumed high-pressure drops on the thermal oil side, minimizing, in this way, the heat exchanger area. A second optimization of the SG was carried out using as strategy the minimization of the heat exchanger area. It is found that the TAC minimization strategy results in savings of around 3.5 M€ throughout the plant lifetime.

Table 3
Proposed designs of heat exchangers.

Parameter	Superheater	Reheater	Preheater	Evap. Kettle	Evap. Rec. + Drum
Shell diameter, D_s (mm)	880	1130	825	2240/1370[a]	860/1000[b]
Baffle cut, B_c (%)	35	30	34	–	–
Baffle spacing, L_{bc} (mm)	762	606	654	–	–
Tubes ext. diameter, D_t (mm)	19.1	15.9	15.9	15.9	15.9
Tubes int. diameter, D_{ti} (mm)	13.6	12.6	11.7	12.6	12.6
Tube pitch, L_{tp} (mm)	24.8	19.9	20.7	19.9	19.9
Tube layout, θ_{tp} (°)	45	90	90	30	30
Tube passes, N_{tp} (–)	2	2	2	2	2
Tubes number, N_{tt} (–)	419-U	1149-U	527-U	1997-U	754-U
Tube length, L_t (m)	7.51	10.31	11.44	9.18	10.97
Shell thickness, t_s (mm)	16	16	13	135	64
Tubesheet thickness, l_{ts} (mm)	134	75	126	210	131
Mass flow (tube-side), $\dot{m}_t$ (kg/s)	30.9	24.8	30.9	263.5	131.75
Mass flow (shell-side)), $\dot{m}_s$ (kg/s)	263.5	35.1	263.5	–/30.9[c]	163.78/15.47[c]
Flow velocity (tube side), v_t (m/s)	11.13	24.03	0.72	1.38	1.83
Flow velocity (shell side), v_s (m/s)	0.80	0.37	0.91	–	0.16
Convective heat transfer coefficient (tube-side), h_t (W/m^2 °C)	3607.1	992.3	7474.8	2738.1	3484.0
Convective heat transfer coefficient (shell-side), h_s (W/m^2 °C)	1757.3	1303.4	2215.7	17929.0	20326.0
Fouling resistance (tube-side), R_t (°C m^2/W)	8.825e-5	3.53e-4	8.82e-5	2.64e-4	2.64e-4
Fouling resistance (shell-side), R_s (°C m^2/W)	2.64e-4	2.64e-4	2.64e-4	1.76e-4	1.76e-4
Overall heat transfer coefficient, U (W/m^2 °C)	703.5	358	1014.7	929.3	1030.1
Heat exchange area (per shell), A (m2)	377.4	1183.2	602.35	1832.0	826.4
Pressure drop (shell-side), ΔP_s (kPa)	27.7	41.20	51.10	–	9.5/26.94[d]
Pressure drop (tube-side), ΔP_t (kPa)	75.41	87.08	14.02	31.95	59.28
TEMA designation	DHU	CFU	DHU	NKU	NXU
Total number of shells, N_s (–)	2	2	2	2	4/2[e]
Total investment cost, C_{invest} (k €)	247	337	428	773	897

[a] Tube bundle diameter.
[b] Steam drum diameter.
[c] Outlet steam mass flow.
[d] Total pressure drop in recirculation loop.
[e] Number of drums.

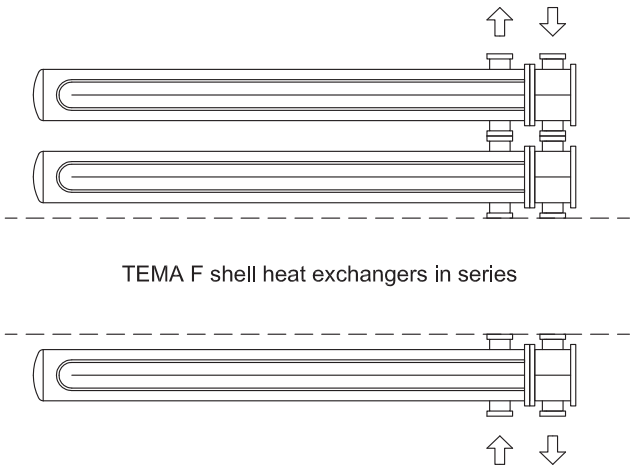

Fig. 9. Proposed design of oil-to-salt heat exchanger with TEMA F shell in series.

5.2. Optimizing the design of the oil-to-salt heat exchanger

The operation of the oil-to-salt heat exchanger determines the temperature drop of the molten salt in the hot tank during charging operation. In addition, it also determines the temperature drop of the thermal oil inlet of the SG during discharging operation. Thermal oil temperature lower than that of nominal conditions decreases the power block efficiency and results in part load operation of the cycle. In order to reduce the power block efficiency penalty, the oil-to-salt heat exchanger is designed with very small approach temperatures, in the range of 3–10 °C [17]. Due to the high heat duty and thermal efficiency required, an oil-to-salt heat exchanger design with TEMA-F shells in series is proposed (see Fig. 9).

The cycle performance during discharging was calculated through an iterative process. First, an energy balance for each heat exchanger of the SG is defined with an initial thermal oil inlet temperature. The thermal oil mass flow is determined by the nominal conditions. The inlet pressure of the turbine is calculated until the live steam mass flow and the heat duties in the water/steam side are balanced. The power of the turbine, the power block efficiency and the outlet temperature of last feedwater heater are calculated in each iteration. At this point, the thermal oil outlet temperature of the SG is also calculated. Then, an energy balance in the TES is realized and a new thermal oil inlet temperature to the SG is obtained. The process is repeated until convergence of heat duties and temperatures is reached in the SG and TES. The turbine efficiency was modeled as a function of the inlet mass flow rate, which was calculated using the Stodola correlation [49]. In each heat exchanger, the overall heat transfer coefficient reduction was estimated by raising the tube mass flow reduction ratio to the power of 0.8.

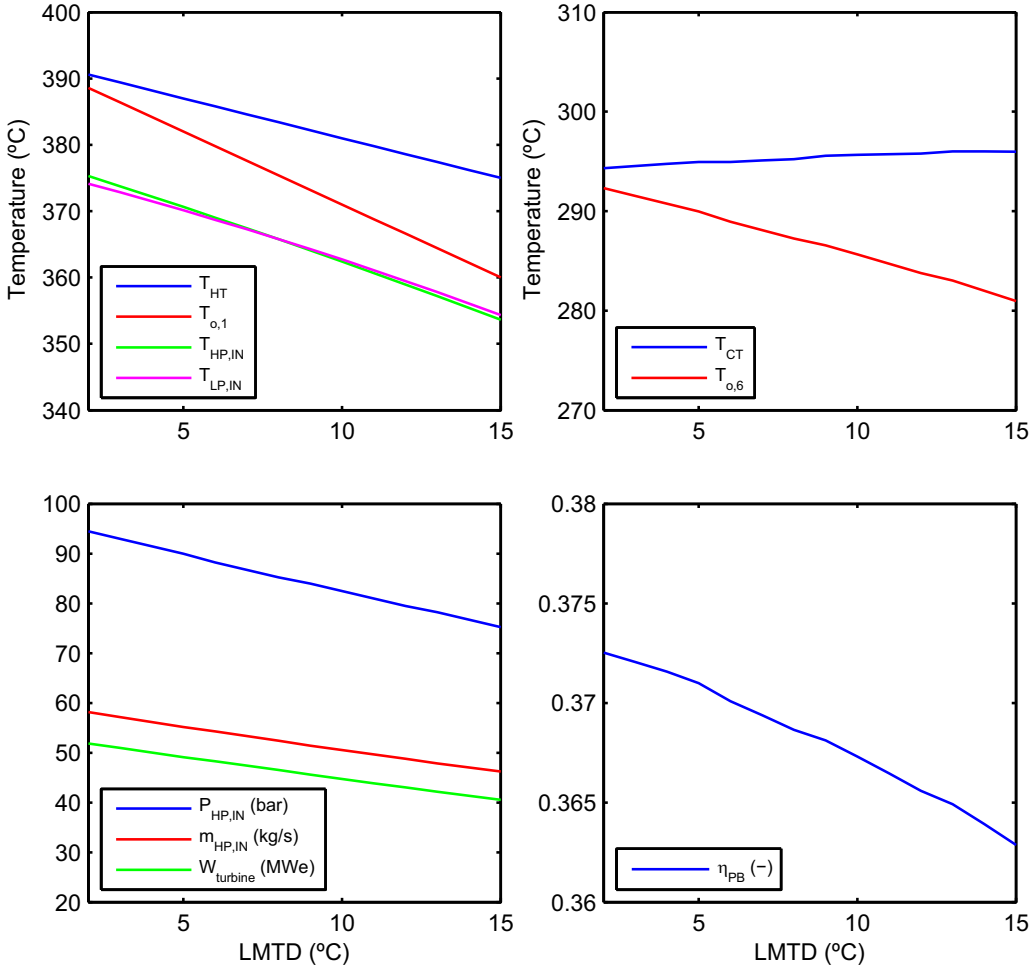

Fig. 10. Power block performance under part load conditions.

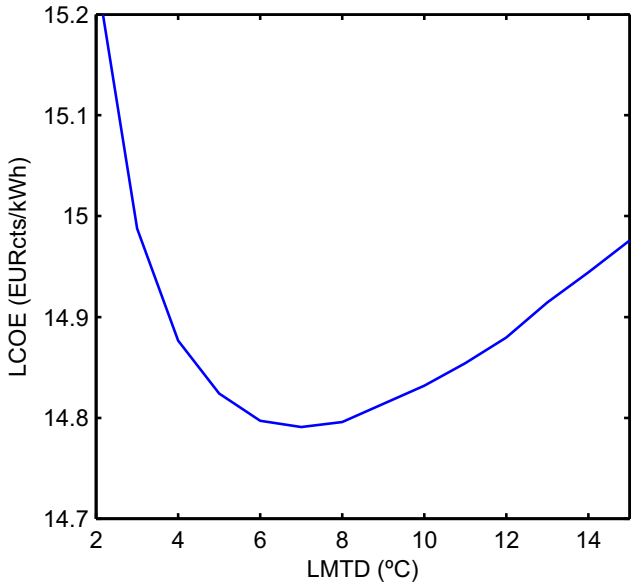

Fig. 11. Economic analysis of the TES.

The initial convergence of the system of equations shows an excess of energy in the preheater of the SG that may lead to steaming. This may induce vibrations, which may trigger tube failure due to two-phase flow through the tubes. Although that may occur in practice, steaming is not allowed in the preheater from an economic point of view [50]. In order to avoid steaming, additional water mass flow is assumed to achieve saturation conditions in the exhaust of the water preheater. In order for the evaporator water level to remain constant, the water excess is circulated to the deaerator.

Table 4
Proposed designs for the oil-to-salt heat exchanger.

Parameter	Design 1	Design 2
Shell diameter, D_s (mm)	2.56	2.56
Baffle cut, B_c (%)	31	32
Baffle spacing, L_{bc} (mm)	1574	1557
Tubes ext. diameter, D_t (mm)	19.1	19.1
Tubes int. diameter, D_{ti} (mm)	14.9	14.9
Tube pitch, L_{tp} (mm)	28.7	28.7
Tube layout, θ_{tp} (°)	45	45
Tube passes, N_{tp} (−)	2	2
Tubes number, N_{tt} (−)	2911-U	2914-U
Tube length, L_t (m)	10	9.5
Number of shells (in series), N_s (−)	6	7
Shell thickness, t_s (mm)	41	41
Tubesheet thickness, l_{ts} (mm)	191	195
Mass flow (tube-side), $\dot{m}_t$ (kg/s)	593	954
Mass flow (shell-side)), $\dot{m}_s$ (kg/s)	954	593
Flow velocity (tube side), v_t (m/s)	1.50	1.00
Flow velocity (shell side), v_s (m/s)	0.55	0.81
Convective heat transfer coefficient (tube-side), h_t (W/m^2 °C)	2892	3073
Convective heat transfer coefficient (shell-side), h_s (W/m^2 °C)	4318	2374
Fouling resistance (tube-side), R_t (°C m^2/W)	2.6e-4	8.8e-5
Fouling resistance (shell-side), R_s (°C m^2/W)	8.8e-5	2.6e-4
Overall heat transfer coefficient, U (W/m^2 °C)	827.76	755.59
Heat exchange area (per shell), A (m2)	3862	3465
Pressure drop (shell-side), ΔP_s (kPa)	612	513
Pressure drop (tube-side), ΔP_t (kPa)	231	373
TEMA designation	NFU	CFU
Total investment cost, C_{invest} (M€)	5.2	5.8

The LCOE of the heat exchanger is calculated for varying LMTD between 2 °C and 15 °C. As seen in Fig. 10, higher values of the LMTD lead to lower power outputs ($W_{turbine}$) and efficiencies (η_{PB}). This is due to the reduced live-steam temperature ($T_{HP,IN}$), inlet pressure ($P_{HP,IN}$) and flow rate ($\dot{m}_{HP,IN}$). As expected, if the outlet temperature of the solar field is kept constant, the hot tank temperature (T_{HT}) decreases with increasing LMTD. On the contrary, the cold tank temperature (T_{CT}) increases with increasing LMTD. This happens because less thermal energy is required in the SG and the decreasing rate of $T_{o,6}$ is smaller than that of $T_{o,1}$.

The results of the economic analysis of the TES of the plant, reveal an optimum LMTD equal to 7 °C (Fig. 11). This agrees well with published work [16]. A small difference is noted because the cost of the oil-to-salt heat exchanger in Ref. [16] was assumed to be approximately 50% lower than in our case.

Because, it was not clear from the beginning which fluid should be placed on the tube side and which on the shell side, two TEMA-F shell designs are analyzed for the oil-to-salt heat exchanger. These designs are presented in Table 4. The pressure on the thermal oil side was set to 20 bar because the vapor pressure of the oil is around 10 bar at 390 °C and the total pressure drop in the SG and the oil-to-salt heat exchanger is approximately 10 bar. In Design 1 the molten salt is placed on the shell side and the thermal oil on the tube side. The opposite is realized in Design 2. Design 1 provides a higher overall heat transfer coefficient than Design 2 that leads to lower heat exchange area and cost. On the other hand, Design 2 may lead to a better drainage operation, since the thermal oil (during charging operation) can melt the molten salt inside the tubes easier.

The heat exchanger designs were evaluated during discharging operation. The first calculations may violate the maximum allowed tube spacing, because a large baffle space is required to fulfill the maximum shell side pressure drop. To avoid vibration problems, a rod type baffle is mounted on the tubes [38]. None of the proposed designs satisfied the maximum shell side pressure drop constraint for TEMA-F shells to prevent thermal leakage. This is because standard single segmental baffle leads to high pressure drops on the shell side. Double or triple segmental baffles can be used as a possible solution to reduce the pressure drop on the shell-side.

6. Conclusions

In this work, the design of the steam generator heat exchangers and the oil-to-salt heat exchanger of a 50 MWe parabolic trough solar power plant was presented and optimized. The optimized design was based on total costs and was obtained using a genetic algorithm with design constraints based on recommended good practice and TEMA standards.

The results show a global optimum for outlet temperature of the thermal oil equal to 293 °C and an evaporator pinch point of 4.85 °C. TEMA-H shells are proposed for the superheater and the preheater, and a TEMA-F shell for the reheater. The reduction of the pressure drop within the steam generator proposed leads to higher savings in the operational cost of the pump of the heat transfer fluid, when compared to other designs reported in literature. Furthermore, a TEMA-X shell recirculation evaporator is proposed, which leads to an important reduction in the shell and tubesheet thicknesses compared with a kettle evaporator. This allows higher temperature gradients in transient regimes.

Lastly, the analysis of the thermal energy storage system revealed an optimum for a logarithmic mean temperature difference of the oil-to-salt heat exchanger of 7 °C. With this temperature difference, two designs were proposed. In the first design the molten salt was placed on the shell side and the thermal oil on the

tube side. The opposite was realized in the second design. The first design is considered the best option, since it was found to have a lower investment cost.

Acknowledgements

This work was supported by project ENE-2015-69486-R of the Ministerio de Economía y Competitividad. Also, D. S. would like to thank the support of Mr. Mikel Ezcurra and Mr. Iñaki Ugarte from Lointek to obtain this grant. F.P. would like to thank the Universidad Carlos III de Madrid, the European Union's Seventh Framework Programme for research, technological development and demonstration (grant agreement no 600371), the Ministerio de Economía y Competitividad (COFUND2014-51509) the Ministerio de Educación, Cultura y Deporte (CEI-15-17) and Banco Santander.

References

[1] Usaola J. Participation of CSP plants in the reserve markets: a new challenge for regulators. Energy Policy 2012;49:562–71. http://dx.doi.org/10.1016/j.enpol.2012.06.060.
[2] National Renewable Energy Laboratory (NREL), 2016. http://www.nrel.gov/csp/solarpaces/by_project.cfm.
[3] Iea. Technology roadmap-solar thermal electricity. 2014. p. 1–52. http://dx.doi.org/10.1007/SpringerReference_7300.
[4] Serna M, Jiménez A. A compact formulation of the Bell–Delaware method for heat exchanger design and optimization. Chem Eng Res Des 2005;83:539–50. http://dx.doi.org/10.1205/cherd.03192.
[5] Ravagnani MA SS, Silva AP, Biscaia EC, Caballero JA. Optimal design of shell-and-tube heat exchangers using particle swarm optimization. Ind Eng Chem Res 2009;48:2927–35. http://dx.doi.org/10.1021/ie800728n.
[6] Mizutani FT, Pessoa FLP, Queiroz EM, Hauan S, Grossmann IE. Mathematical programming model for heat-exchanger network synthesis including detailed heat-exchanger designs. 2. Network synthesis. Ind Eng Chem Res 2003;42:4019–27. http://dx.doi.org/10.1021/ie020965m.
[7] Serth RW, Lestina TG. Process heat transfer: principles, applications and rules. 2014. http://dx.doi.org/10.1016/B978-0-12-397195-1.00005-4.
[8] Hall SG, Ahmad S, Smith R. Capital cost targets for heat exchanger networks comprising mixed material of construction, pressure ratings and exchanger types. Comput Chem Eng 1990;14:319–35.
[9] Seider WD, Seader JD, Lewin DR, Widagdo S. Product and process design principles: synthesis, analysis, and evaluation. 2010.
[10] Taal M. Cost estimation and energy price forecasts for economic evaluation of retrofit projects. Appl Therm Eng 2003;23:1819–35. http://dx.doi.org/10.1016/S1359-4311(03)00136-4.
[11] Purohit GP. Estimating cost of shell and tube heat exchangers. Chem Eng 1983;90:57–67.
[12] Willdi PT. Minimizing shell-and-tube heat exchanger cost with genetic algorithms and considering maintenance. Int J Energy Res 2007;31:867–85. http://dx.doi.org/10.1002/er.
[13] Ponce-Ortega JM, Serna-González M, Jiménez-Gutiérrez A. Use of genetic algorithms for the optimal design of shell-and-tube heat exchangers. Appl Therm Eng 2009;29:203–9. http://dx.doi.org/10.1016/j.applthermaleng.2007.06.040.
[14] Fettaka S, Thibault J, Gupta Y. Design of shell-and-tube heat exchangers using multiobjective optimization. Int J Heat Mass Transf 2013;60:343–54. http://dx.doi.org/10.1016/j.ijheatmasstransfer.2012.12.047.
[15] Kelly B. Nexant parabolic trough solar power plant systems analysis task 1: preferred plant size. Contract. 2006.
[16] Kelly B, Kearney D. Thermal storage commercial plant design study for a 2-tank indirect molten salt system final report. 2006.
[17] Herrmann U, Kelly B, Price H. Two-tank molten salt storage for parabolic trough solar power plants. Energy 2004;29:883–93. http://dx.doi.org/10.1016/S0360-5442(03)00193-2.
[18] Zaversky F, Sánchez M, Astrain D. Object-oriented modeling for the transient response simulation of multi-pass shell-and-tube heat exchangers as applied in active indirect thermal energy storage systems for concentrated solar power. Energy 2014;65:647–64. http://dx.doi.org/10.1016/j.energy.2013.11.070.
[19] Taborek JWP, Palen JJW, Taborek J. Solution of shell side flow pressure drop and heat transfer by stream analysis method. Chem Eng Prog Symp Series 1969;65:53–63.
[20] ESDU. Baffled shell-and-tube heat exchangers: flow distribution, pressure drop and heat transfer coefficient on the shellside. ESDU Int Ltd.; 1983. No. 83038.
[21] Palen JW. Shell and tube reboilers. In: Heat exchanger design handbook. New York: Hemisphere Publishing Corp; 1988.
[22] Swanson LW, Palen JW. Convective boiling applications in shell-and-tube heat exchangers. Intl. conf. convective flow boiling. 1995.
[23] Smith R. Chemical process design and integration. John Wiley & Sons; 2005.
[24] Wagner SJ, Rubin ES. Economic implications of thermal energy storage for concentrated solar thermal power. Renew Energy 2014;61:81–95. http://dx.doi.org/10.1016/j.renene.2012.08.013.
[25] Montes MJJ, Abánades A, Martínez-Val JMM, Valdés M. Solar multiple optimization for a solar-only thermal power plant, using oil as heat transfer fluid in the parabolic trough collectors. Sol Energy 2009;83:2165–76. http://dx.doi.org/10.1016/j.solener.2009.08.010.
[26] Version SAM. Solar advisor model reference manual for CSP trough systems. 2009.
[27] Guédez R, Spelling J, Laumert B. Reducing the number of turbine starts in concentrating solar power plants through the integration of thermal energy storage. J Sol Energy Eng 2014;137:11003. http://dx.doi.org/10.1115/1.4028004.
[28] Garland WJ, Hand BJ. Simple functions for the fast approximation of light water thermodynamic properties. Nucl Eng Des 1989;113:21–34. http://dx.doi.org/10.1016/0029-5493(89)90293-8.
[29] Byrne RC, Tema, York N, Byrne RC. Standards of the tubular exchangers manufacturers association. Main. 2007.
[30] Zavoico AB. Solar power tower - design basis document. Sandia Natl Lab; 2001. p. 148. http://dx.doi.org/10.2172/786629.
[31] Mukherjee R. Practical thermal design of shell-and-tube heat exchangers. 2004.
[32] Thulukkanam K. Heat exchanger design handbook. second ed. 2013. http://dx.doi.org/10.1201/b14877.
[33] Mukherjee R. Does your application call for an F-Shell heat exchanger? CEP Mag 2004:40–5.
[34] Bradshaw RW, Dawson DB, De la Rosa W, Gilbert R, Goods SH, Hale MJ, et al. Final test and evaluation results from the solar two project. Sandia Natl Lab 2002:294. http://dx.doi.org/10.2172/793226.
[35] Aalborg CSP. Aalborg CSP concentrated solar power steam generators. 2016. http://www.aalborgcsp.com.
[36] Kolb GJ. An evaluation of possible next-generation high-temperature molten-salt power towers. 2011. p. 1–120. doi:SAND20011-9320.
[37] Mukherjee R. Effectively design shell-and-tube heat exchanger. Chem Eng Prog 1998:17.
[38] Shah R, Sekulic D. Fundamentals of heat exchangers design. 2003.
[39] Kreith F. The CRC handbook of thermal engineering. Boca Raton: LLC CRC Press; 2000.
[40] Caputo AC, Pelagagge PM, Salini P. Joint economic optimization of heat exchanger design and maintenance policy. Appl Therm Eng 2011;31:1381–92. http://dx.doi.org/10.1016/j.applthermaleng.2010.12.033.
[41] Merritt C. Process steam systems: a practical guide for operator, maintainer and designers. Hoboken, New Jersey: John Wiley & Sons; 2015.
[42] Taborek J. Shell and tube heat exchangers: single phase flow. In: Heat exchanger design handbook. New York: Hemisphere Publishing Corp; 1983.
[43] Fauske HK. Contribution to the theory of two-phase one-component critical flow. Argonne Natl Lab Rep; 1962. ANL-6333. doi:Report ANL-6633.
[44] Kim Y-S. A proposed correlation for critical flow rate of water flow. Nucl Eng Technol 2015;47:135–8. http://dx.doi.org/10.1016/j.net.2014.11.004.
[45] Ganapathy V. Understanding boiler circulation. Chem Eng 2013:52–6.
[46] C. A. D. Andalucía, 43.321/05, Solicitud de aprobación del proyecto de ejecución, y declaración en concreto de la utilidad pública del proyecto Andasol-1., Boletin oficial del Estado, Gobierno de España.
[47] Lebrija 1: international solar thermal reference. Energ Int 2012;123:36–44.
[48] Yang Y, Wang Z, Xu E, Ma G, An Q. Analysis and optimization of the start-up process based on badaling solar power tower plant. Energy Proced 2015;69:1688–95. http://dx.doi.org/10.1016/j.egypro.2015.03.130.
[49] Stodola A, Lowenstein LC. Steam and gas turbines, vol. I. New York: McGraw-Hill Book Company; 1945.
[50] Sarkar D. Thermal power plant: design and operation. Elsevier Inc.; 2013.